Energy Harvesting Photovoltaic System to Charge a Cell Phone in Indoor Environments

Jayme Milanezi Junior, Ronaldo S. Ferreira Junior, João Paulo C. L. da Costa, Marco A. M. Marinho, Rafael A. Shayani and Rafael T. de Sousa Junior
Laboratory of Array Signal Processing (LASP)
Department of Electrical Engineering
University of Brasilia
Braslilia-DF, Brazil 55-61-2192-8079
www.pgea.unb.br/∼ lasp
Email: jmilanezi@gmail.com, ronaldojr@aluno.unb.br, joaopaulo.dacosta@ene.unb.br, marco.marinho@ieee.org, shayani@ene.unb.br, desousa@unb.br

***Abstract*—Research advances in materials science improved gradually photovoltaic systems efficiency. However, such systems are limited to work in the presence of sun light, and they also depend on the geographic localization and on the period of the year, usually limited to 6 to 8 hours a day. In order to take maximum advantage of solar panels, it is crucial to use them also in cloudy weather or even at night. Therefore, in this paper, we propose to recycle light energy from artificial light sources to enable the use photovoltaic systems along 24 hours a day. We validate our proposal by means of measurements performed using artificial light in indoor environments. As a practical result, we show that 7 hours recharging in an indoor environments implies in 94.08 % of the overall cell phone battery capacity. Furthermore, we also propose a circuit for charging of a battery of a cell phone.**

I. Introduction

Nowadays, it has become significantly important to exploit novel power resources, as overall energetic demands grows faster than production, especially near large urban centers. Another relevant fact is that power generating near consumption area leverages economic benefits concerning infrastructure, postponing investments as much as lowering losses. The whole electrical supply chain, which in many countries is partially financed by public budget, is freed from parcels of mandatory investments along the involved assets in power generation and distribution. If houses and offices generate partially their power, it is expected that the overall power demand from the commercial supply grid would be lowered.

There are many sources of energy that are not, or barely, used for power generation. According to [1] and [2], technical aspects enable luminous energy to be one of the most promising power sources, given that their power density related to area or volume is among the highest ones. In a outdoor environment, at noon, the ratio of available energy for a solar cell reaches 15 $m\mathrm{W}/\mathrm{cm}^2$.

On the other hand, a small piezoelectric generator using shoes movements achieves $330\mu\mathrm{W}/\mathrm{cm}^3$; a thermoelectric generator (10 °C gradient) produces about $40\mu\mathrm{W}/\mathrm{cm}^3$; acoustic noise generator (100 dB) falls short of $1\mu\mathrm{W}/\mathrm{cm}^3$ [1].

We evaluate if luminous energy from artificial light constitutes a potentially exploitable source in terms of harvesting systems. According to [3], the harvesting involving indoor environment provides 3 orders of magnitude lower than outdoor environment. In recent publications [3], [4], [5], [6], [7], [8], [9], [10], [11] there has been an increasing interest in energy harvesting in indoor environments. However, in [4], [5], [6], [7], [11], [12], [13], [14], the goal was supplying a sensor node. Due to the importance of charging portable electronic devices, in this paper, we perform measurements in order to verify the possibility of supplying the battery of a cell phone using artificial light. As an additional contribution, we also propose a circuit to charge a cell phone using artificial light and we show the efficiency of our proposed circuit by means of simulations.

The remainder of this paper is organized as follows: Section II presents a state-of-the-art overview. Section III reports results over measurements undertaken in indoor environments for the solar panel in order to feature its open voltage circuit and short circuit current at low light levels. Profile of storage energy, cycles of charging and discharging of cell phone battery are presented in Section IV. Section V discusses an indoor experiment implemented to probe cell phone charging capacity over the utilization of the solar panel, using indoor artificial light and counting on an interposed boost converter circuit; Section VI concludes the paper.

II. State-of-the-art overview

According to [3], photovoltaic devices are classically optimized for the solar spectrum. Energy-efficient fluorescent and LED lighting have largely replaced incandescent light bulbs, so that the spectral profile of artificial light has changed from broad spectra, originated by low temperature blackbodies, to sharply peaked narrow spectra. Table II presents a comparison between crystalline Silicon (c-Si), amorphous Silicon (a-Si) and P3HT/PCBM bulk heterojunctions organic PV (OPV) panels in experiments with light from solar light, Compact Fluorescent Lamp (CFL), Cold-Cathode Fluorescent Lamp (CCFL) and LED [3]. Based on Table I, an a-Si solar panel is more suitable for indoor artificial light in comparison with other types of panels.

In [6], an amorphous silicon photovoltaic cell (PV) has a relatively high efficiency at low light intensity levels compared

978-1-4799-2516-2/14/$31.00 ©2014 IEEE

Table I. MAXIMAL EFFICIENCY VALUES FOR CRYSTALLINE SILICON, AMORPHOUS SILICON, AND ORGANIC BHJ SOLAR CELLS UNDER DIFFERENT SPECTRAL ILLUMINATION [3].

		Luminous		Source	
		Solar	CFL	CCFL	LED
PV Material	crystalline-Si	49 %	50 %	52 %	54 %
	amorphous-Si	37 %	74 %	70 %	80 %
	OPV	28 %	63 %	59 %	63 %

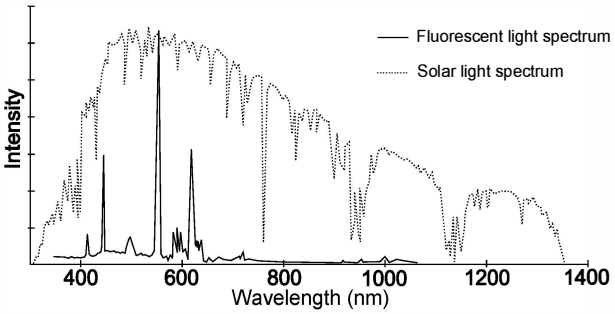

Figure 1. Typical solar light AM 1.5 and cold-cathode fluorescent light spectra.

to other types of cells. Such property makes them particularly suitable for indoor and low power light environments. Other types of panel, as c-Si, have higher performance in an outdoor environment compared to the indoor environments due to the scarce spectrum of the artificial light as exemplified in Figure 1 [3].

III. OPEN CIRCUIT AND SHORT CIRCUIT MEASUREMENTS IN INDOOR ENVIRONMENTS FOR THE A-SI SOLAR PANEL

In this section, measurements were performed with the a-Si solar panel with no load connected to it. Our focus here is to observe only the behavior of the a-Si solar panel using indoor artificial light.

Given that incandescent light bulbs are falling into disuse in many countries, in this paper, only fluorescent and LED lamps are considered. This factor was determinant for choosing a-Si panel, since it offers a higher efficiency to produce power from such spectrum as shown in the previous section. Another reason to choose a-Si panel lies on its low cost. From now on, all presented results were obtained by means of measurements obtained in our laboratory.

A panel of amorphous Silicon (a-Si) with maximum current $I_{\max}$ = 200 mA and maximum voltage $V_{\max}$ = 6 V and with size of 95 mm x 110 mm is employed in the experiments of this paper. Over 54 measurements were performed with the a-Si panel being under different light intensity levels. The variables of interest are open circuit voltage, $V_{\rm oc}$, and short circuit current, $I_{\rm sc}$, in function of incident lux $L_{\rm x}$. A white 8 W LED light bulb (color temperature 4.700 K) was used for the measurements. Figures 2 and 3 show the curves obtained during the measurements. Intensity and spectrum of light were kept constant, whereas distance between panel and LED was varied, in order to provide several light intensity levels.

From the curves of Figs. 2 and 3, (1) and (2) can be written with the relationship between $V_{\rm oc}$ and $L_{\rm x}$ and between $I_{\rm sc}$ and $L_{\rm x}$:

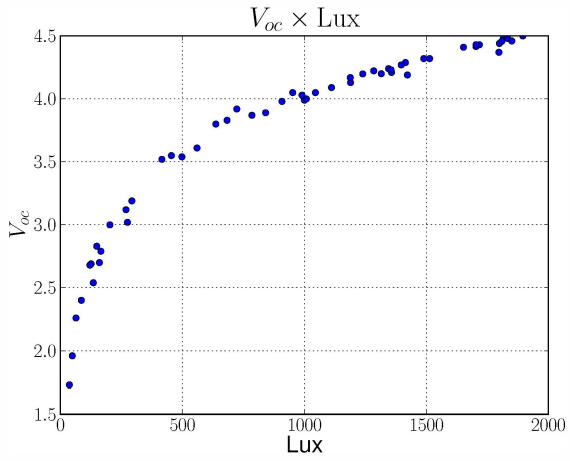

Figure 2. Absorbed Light Intensity ($L_{\rm x}$) versus Open Circuit Voltage ($V_{\rm oc}$) of the solar panel 95 mm x 110 mm for a LED 8 W lamp.

$$\mathrm{V_{oc}} = -0.68789 + 0.68159 \cdot ln(\mathrm{L_x}), (1)$$

$$\mathrm{I_{sc}} = 0.00074 + 0.00084 L_{\rm x}. \ (2)$$

, where $\ln(\cdot)$ is the natural logarithm operator.

From (1) and (2) we obtain values of the coefficient of determination (R^2), respectively, equal to 99.52 % and 99.65 %. Therefore, both equations have a very good approximation with the curves in Figs. 2 and 3. Significance of the independent variables are 0.01 % in either cases. Significance and coefficient of determination were obtained by means of linear regression, which comprises the principle of residuals normality. All over this paper, the obtained data samples bore this principle, which is also understood as the variance constancy, or homocedasticity.

Inverting terms in (1) results in $(\mathrm{L_x}) = 1.0092 \cdot e^{1.46716 \cdot V_{\bullet c}}$. Since solar cells are voltage limited current sources, the relation between the light intensity $L_{\rm x}$ versus short circuit current ($I_{\rm sc}$) is linear as shown in Figure 3.

IV. CHARGE PROFILE OF A CELL PHONE BATTERY

In this section, measurements are performed connecting the cell phone directly to the power outlet through its charger. Our focus here is to identify the behavior of the battery.

Experiments in this paper employed a Samsung B3210 cell phone, that uses a 800 mAh Lithium-Ion rechargeable battery. The battery was initially completely discharged in order to recharge it using an electrical socket from the electrical power system, whose output is 220 V in 60 Hz.

The whole process comprises a four-charging regime [15]: the first stage corresponds to a constant current charge while voltage increases; the second stage is related to the saturation, when voltage stabilizes whereas the current lowers; the third phase is cut-off, voltage decays softly. Finally, the stand-by

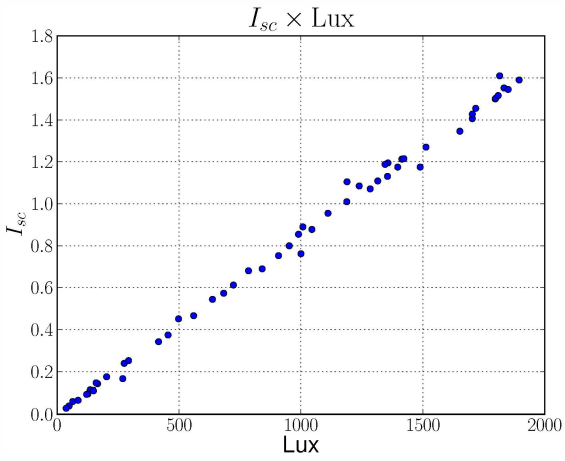

Figure 3. Absorbed Light Intensity (L_x) versus Short Circuit Current (I_{sc}) of a solar panel 95 mm x 110 mm for a LED 8 W lamp.

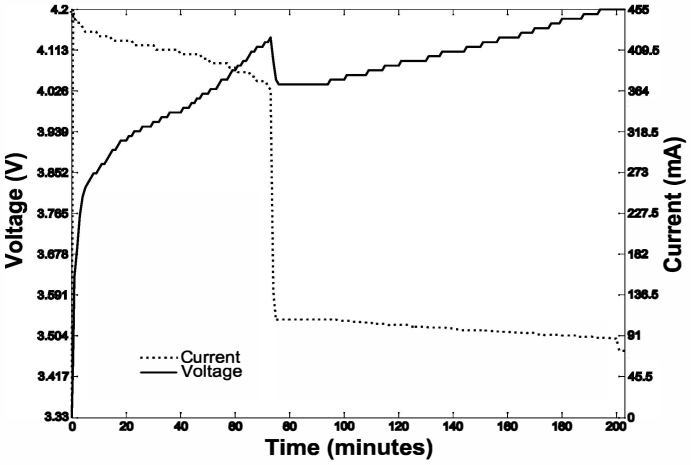

Figure 4. Current and voltage versus time of a cell phone charging at 220 V, 60 Hz.

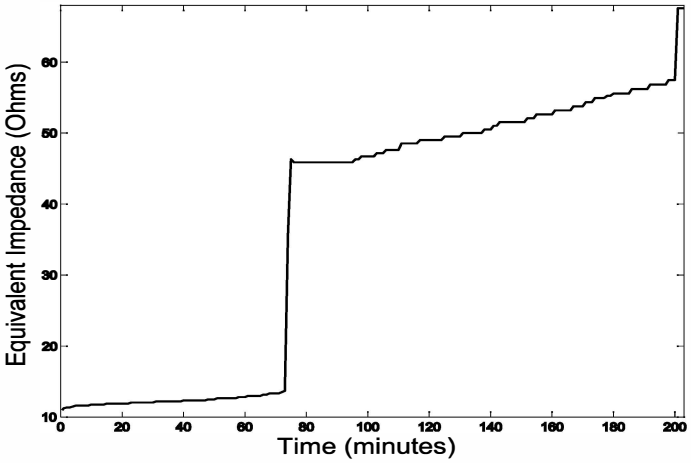

Figure 5. Apparent Impedance (Ω) of cell phone seen by the source.

mode occurs when the battery draws a low-level current from the source in order to recuperate voltage after some charge leakage. At the beginning of the charging process, the current is maximum and decreases until a time instant in which the current falls abruptely, when the second stage starts. These two first stages are pictured in Figure 4.

At first, current underwent a linear decay, until the 73^{rd} minute. Thereafter, it obeyed to another linear expression, corresponding to the less steeper descendent along lower values (saturation). The expression of current I as a function of time t in minutes is given by expressions (3) and (4). The times instants were taken at each minute. At each time instant, the current and the voltage were measured, making possible to calculate the instantaneous transfer power. Cell phone was kept turned off during the entire process.

$$For\ 0 \leq t \leq 73, I = -0.859t + 439.71, \quad (3)$$

$$For\ 74 \leq t \leq 203, I = -0.194t + 111.26. \quad (4)$$

The approximation error in terms of determination coefficients R^2 for expressions (3) and (4) are, respectively, 95.59 % and 99.07 %.

The internal control system of the cell phone manages the input voltage from the DC source, which delivers 5 V all the time. The first stage comprises an increasing voltage regime, as the current is managed to stay in a narrow set of values by the control system. When the voltage achieves approximately 4.15 V, this system steps in to reduce the current towards lower levels, avoiding damages. This moment corresponds to the observed discontinuity over voltage and current values, when the second phase of charging the battery begins. This is in accordance with Figure 4.

The cell phone internal circuit control aims to preserve the battery physical safety, since the chemical structure of the Li-ion battery does not allow overcharging [15]. Considering the profiles of current and voltage as observed above, it is possible to imagine that there is an equivalent R which is not constant and might replace the entire cell phone, in order to produce the same final circuit current. Hence, the cell phone could be substituted by a black box, into which there is a time-variable resistance whose value increases as the stored energy arises, due to the behavior of the cell internal control system. The higher the internal voltage source of the battery, the higher is the apparent equivalent resistance, which has the behavior shown in Figure 5. This is based on a mathematical rather than a physical comparison, which nevertheless bears concrete results into the modeled circuit. The instantaneous values of this variable impedance were obtained by the division of voltage upon current. The expression for R in function of time, in the right part of graph (from the 75^{th} minute on), is now $R = 44.713e^{0.002t}$.

In Figure 6, the instantaneous values of delivered power were obtained by multiplying the current by the voltage of 5 V, which is delivered from the outlet. Therefore, Figure 6 depicts the entire power tranferred to the cell phone, instead of its battery. This was made to visualize in which conditions such transferring power would be more effective, since we consider that the external voltage source, either the outlet or the boost converter associated with the a-Si PV panel, is supposed to deliver 5 V all the time.

One may notice that the most favourable situation to transfer energy to the cell phone occurs in the final part of the

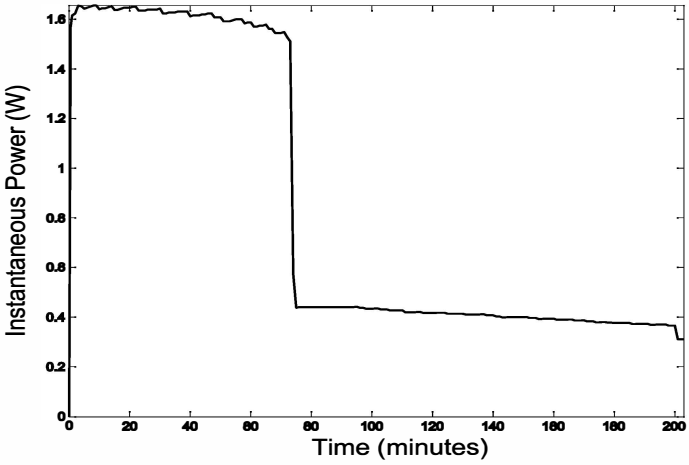

Figure 6. Instantaneous transferred power to the cell phone seen by the source.

saturation stage. Since the apparent impedance arises, the cell phone will draw a lower current, diminishing the probability of voltage to plunge, considering that the source is a solar panel. Hence, hereafter we adopt the premise according which the higher is the energy stored in the battery (higher equivalent impedance), the more effective will be the power transfer. This corresponds to the right part of the graphic shown in Figure 6. Furthermore, the PV panel has a higher internal impedance, and such characteristic offers the possibility of increasing the impedance load and the power simultaneously.

V. Indoor Experiment Using Artificial Light

In this experiment, the cell phone is charged considering indoor light. In order to perform measurements in indoor scenarios, the environment in Figure 7 is suggested. This figure shows an office-desk with a lamp in its support. The a-Si panel was installed on the bottom of the lamp support, inside of which an 8 W LED lamp was installed to provide artificial light. The center of the LED lamp was considered to be apart 13 cm from one of the panel borders. The cell phone is connected to the solar panel and a boost converter, using it as its charger, in the same way while charging it directly by the grid.

An enlarged solar panel, which delivers 2.8 V ($V_{\rm i}$) and power of 3.92 W at lower luminosities, was considered. These hypothetical values for the panel aim to allow the examination of possible results in the recycling process. Considering the environment of Figure 7, light beams must to be directed to the plan of the desk and not to the panel, since the charging process should not disturb the usage of the desk for reading and other activities.

A boost converter was designed and simulated in order to step up the solar panel voltage allowing the battery charge. Figures 8 shows the circuit designed to charge capacitor and Figure 9 shows the evolution of voltage and current over the boost output. According to [16], the commercial available boost converters use recommended capacitor and inductors values, stated in the datasheets. This simple boost converter was designed with an oscillator of 200 kHz whose duty cycle is 80% (D = 0.8), since $V_{\rm out}$ is 5 V, therefore five times the value of $V_{\rm i}$.

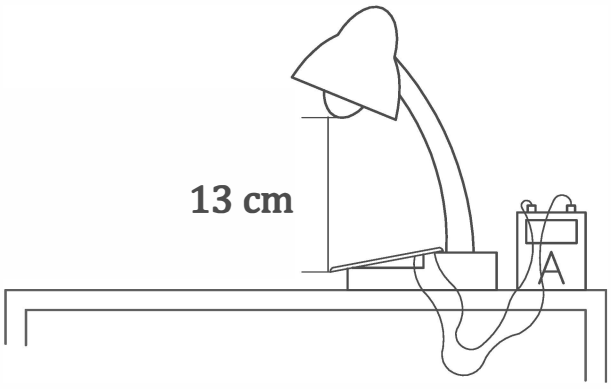

Figure 7. Overall deployment of cell phone, ammeter (in series) and solar panel under a light-support in an office for electrical current measurement.

The cell phone will only behave as a valid load when the boost output voltage is around 4.7 V - 5 V; below those voltage levels, it is likely to behave as an open circuit. Given the constraint of 2.8 V output voltage, we estimate more accurately the value of L in order to achieve the amount of power that the panel should furnish, which is 3.92 W, as well as to determine the oscillator frequency. The critical inductance is defined as the inductance at the boundary edge between continuous and discontinuous modes and is defined as (5).

$$L > \frac{V_{\rm inmin} \cdot (V_{\rm out} - V_{\rm min})}{F_{\rm sw} \cdot I_{\rm out} \cdot V_{\rm out}^2}[H] \tag{5}$$

In (5), $V_{\rm inmin}$ is the minimum input voltage, $V_{\rm out}$ is the desired output voltage, $I_{\rm out}$ corresponds to the desired maximum output current; $F_{\rm sw}$ is the switching frequency of the converter, and $K_{\rm ind}$ is the estimated coefficient that represents the amount of inductor ripple current relative to the maximum output current. A good estimation for the inductor ripple current is 20% to 40% of the output current, that is, $0.2 < K_{\rm ind} < 0.4$. Considering feeding cell phone with power, $V_{\rm out}$ = 5 V. It was adopted $K_{\rm ind}$ = 0.3, $F_{\rm sw}$ = 200 kHz and $V_{\rm inmin}$ = 1.0 V, with $I_{\rm out}$ = 100 mA. The resultant minimum value is 26 μH. If our choice for $V_{\rm inmin}$ is 1.16 V, then the minimum L is 32 μH. These observations allow us to employ an inductor of 33 μH.

According to [17], since the capacitors equivalent series resistance (ESR) affects efficiency, low-ESR capacitors will be used for best performance. A load resistance of 50 Ω was adopted, according to the verified values for R in the beginning of the second stage of Figure 5. An approximate expression for the required capacitance as a function of ripple voltage requirement, $\Delta {\rm V}_{\rm out}$, D, switching frequency $F_{\rm s}$ and output voltage, $V_{\rm out}$ is given by

$$C \geq \frac{V_{\rm out} \cdot D}{F_{\rm s} \cdot \Delta V_{\rm out} \cdot R}. \tag{6}$$

Considering $\Delta {\rm V}_{\rm out}$, which is maximum ripple output voltage, as 5% (or 0.05), assuring the minimum output voltage to stay on 4.75 V, the minimum value of output capacitor is 8 μF. Therefore, it is possible to choose $C2$ to be 20 μF.

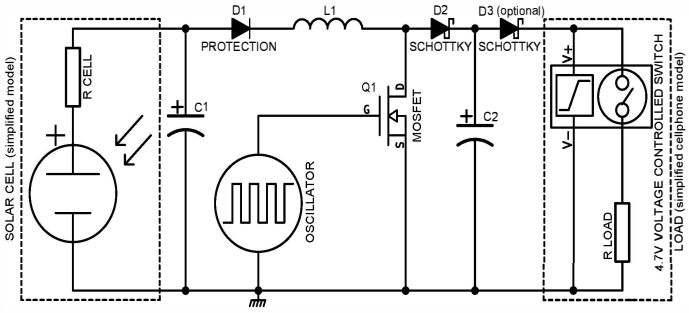

Figure 8. Designed boost converter producing 5 V in steady state

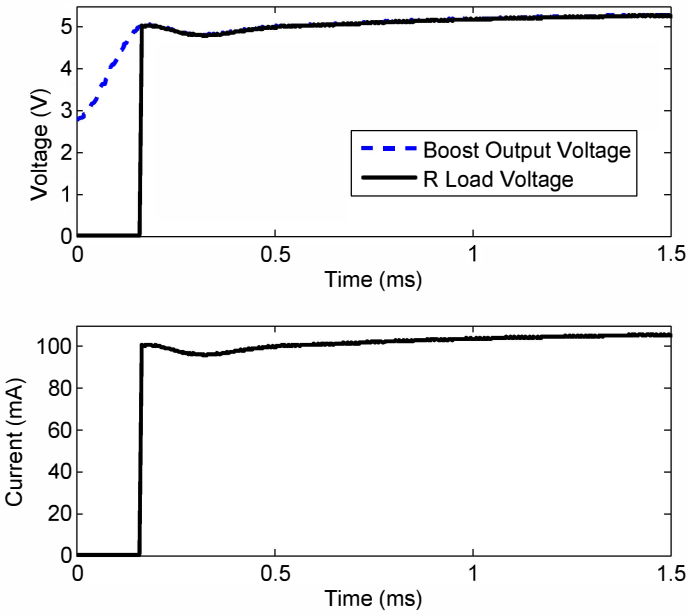

Figure 9. Effective voltage and current in steady state over a load of resistance R of 50 Ω.

The constant RC, shown in (7), requires commonly a higher value for resultant C in order to avoid the deterioration of voltage value. But, with these values of R and $C2$, even when $C1$ equals 100 μF the result makes I_{out} to decay less than 0.5%. Considering that low levels of resistance load might demand higher capacitances in order to avoid I_{out} to lower significantly, the value of $C1$ is chosen to be 100 μF.

$$i_c = \frac{E}{R} e^{-\frac{t}{RC}} \tag{7}$$

Figure 8 depicts this simple boost converter circuit. The hypothetical resistance R is inserted. in Figure 9, the performance of the circuit is shown.

Figure 9 depicts the blue line which represents the boost output voltage, whereas the black line shows the effective values of voltage and current absorbed by the cell phone.

Considering the conditions of the boost and the panel, which must provide 2.8 V minimum, the time to achieve steady state does not overcome 0.3 ms.

In a limited voltage current source, as the solar panel, in the flat part of the V x I graphic, the bulkier the resistance

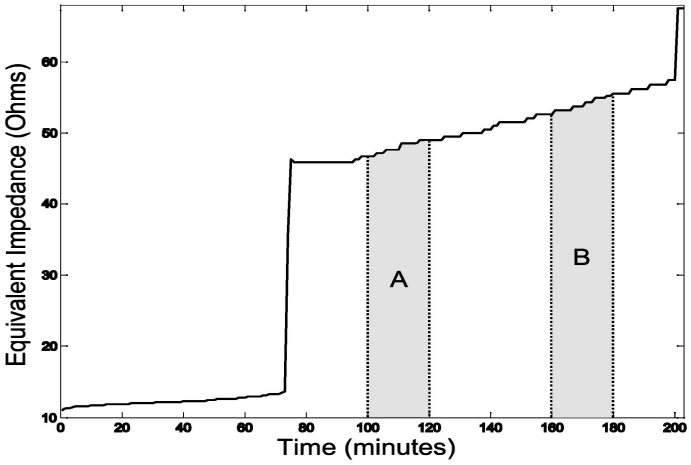

Figure 10. Figure 5 with bars indicating equal periods of time A and B as demonstration that transferred power is influenced by resistance (PB>PA).

coupled, the higher is the power transferred to load. If power is RI^2, then it is interesting to supply load with higher values of resistance, since it does not make voltage to drop excessively. According to Figure 5, R increases when full charge of the cell phone has just been completed. Figure 10 is in accordance with Figure 5 showing that during the period 'A', the battery will receive less energy than during period 'B', considering equal durations.

According to our simulations, about 0.5 W can be transmitted to the battery steadily, day and night, since illumination over day hours is fairly more intense than by nights. It can be noticed that in just one day (24 hours) the proposed system can return 12 Wh to a battery, which overcome the overall energy needed to its full charge, which is approximately 3.72 mWh. Much more than this can be achieved by just making smaller the distance between lamp and the a-Si panel: with 1.5 cm less between panel and LED lamp, current increased 36 % and, therefore, 85 % in power.

Considering again our cell phone receiving energy, if only nights are considered, at the end of one week, recharging the device along 7 hours during each night, energy sent achieves 3.5 mWh, meaning 94.08 % of the whole energetic need of the device. Considering buildings that keep their lamps with lights on 24 hours, turning these energetic profits into more likely goals, three cell phones could have their batteries fully recharged daily.

VI. Conclusion

There are in the literature works related to the recycling of artificial light in indoor environments in order to recharge sensor nodes. To the best of our knowledge, no experiment has been conducted until now in order to recharge batteries of electronic devices using artificial light in indoor environments or at night.

In this paper, we proposed to recycle the light energy from lamps and other artificial light sources in order to use photovoltaic systems 24 hours a day. We validate our proposal by comparing measurements performed using sun light and measurements performed using artificial light in an indoor environment.

As a practical result, we show that 7 hours recharging in an indoor environment results in 94.08 % of the overall battery capacity. The efficiency of our proposed circuit is proven by means of simulations.

REFERENCES

[1] Q. I. Ali, Design & implementation of a mobile phone charging system based on solar energy harvesting, in: EPC-IQ 2010, 2010, pp. 264–267.

[2] J. A. Paradiso, T. Starner, Energy scavenging for mobile and wireless electronics, Pervasive Computing, IEEE 4 (2005) 18–27.

[3] Y. Afsar, J. Sarik, M. Gorlatova, G. Zussman, I. Kymissis, Evaluating photovoltaic performance indoors, in: 2012 38th IEEE Photovoltaic Specialists Conference (PVSC), 2012, pp. 1948–1951.

[4] M. Gorlatova, A. Wallwater, G. Zussman, Networking low-power energy harvesting devices: Measurements and algorithms, in: 2011 Proceedings IEEE INFOCOM, 2011, pp. 1602–1610.

[5] A. S. Weddell, G. V. Merrett, , B. M. Al-Hashimi, Ultra low-power photovoltaic MPPT technique for indoor and outdoor wireless sensor nodes, in: Design, Automation & Test in Europe Conference & Exhibition (DATE), 2011, 2011, pp. 1–4.

[6] H. Yu, Q. Yue, H. Wu, Power management and energy harvesting for indoor photovoltaic cells system, in: 2011 Second International Conference on Mechanic Automation and Control Engineering (MACE), 2011, pp. 521–524.

[7] C. Carvalho, J. P. Oliveira, N. Paulino, Survey and analysis of the design issues of a low cost micro power dc-dc step up converter for indoor light energy harvesting applications, in: 2012 Proceedings of the 19th International Conference Mixed Design of Integrated Circuits and Systems (MIXDES), 2012, pp. 455–460.

[8] A. Somov, R. P. C. C. Ho, J. W. Evans, P. K.Wright, Printed electrochemical capacitors for energy scavenging sensor networks, in: Networked Sensing Systems (INSS), 2012 Ninth International Conference on, 2012, pp. 1–6.

[9] D. S. Ha, Small scale energy harvesting - principles, practices and future trends, in: 2011 IEEE 14th International Symposium on Design and Diagnostics of Electronic Circuits & Systems (DDECS), 2011, pp. 1–1.

[10] L. Huang, W. Rieutort-Louis, Y. Hu, J. Sanz-Robinson, S. Wagner, J. C. Sturm, N. Verma, Integrated all-silicon thin-film power electronics on flexible sheets for ubiquitous wireless charging stations based on solar energy harvesting, in: 2012 Symposium on VLSI Circuits (VLSIC), 2012, pp. 198–199.

[11] Y. K. Tan, S. K. Panda, Energy harvesting from hybrid indoor ambient light and thermal energy sources for enhanced performance of wireless sensor nodes, IEEE Transactions on Industrial Electronics 58 (2011) 4424–4435.

[12] H. Yu, H. Wu, Y. Wen, An ultra-low input voltage power management circuit for indoor micro-light energy harvesting system, in: Sensors, 2010 IEEE, 2010, pp. 261–264.

[13] K.-J. Park, S.-M. Kang, H. S. Kim, C.-W. Baek, T. K. Chung, Energy scavenging system utilizing mems switch for power management, Electronics Letters 48 (2012) 948–949.

[14] N. J. Guilar, T. J. Kleeburg, D. R. Y. A. Chen, R. Amirtharajah, Integrated solar energy harvesting and storage, IEEE Transactions on Very Large Sacle Integration (VLSI) Systems 17 (2009) 627–637.

[15] http://batteryuniversity.com/learn/article/charging_lithium_ion_batteries (November 2013).

[16] M. Green, Design calculations for buck-boost converters, Texas Instruments Inc.

[17] B. M. Hasaneen, A. A. E. Mohammed, Design and simulation of DC/DC boost converter, Selected Works.